scientific reports

Check for updates

OPEN

Mitigating fines migration in low salinity water flooding of clay rich sandstones using TiO_2 Saponin Zr nanocomposites

Yuman Li[1]✉, Farag M. A. Altalbawy[2], Nikunj Rachchh[3], T. Ramachandran[4], Aman Shankhyan[5], A. Karthikeyan[6], Dhirendra Nath Thatoi[7], Deepak Gupta[8,9], Mohammad R. K. M. Al-Badkubi[10,11,12], Dilsora Abduvalieva[13], Samim Sherzod[14]✉ & Mohammad Mahtab Alam[15]

Mitigating formation damage due to fines migration is crucial for maintaining reservoir productivity in enhanced oil recovery (EOR) processes. This research introduces a novel composite, Titanium dioxide nanoparticles coated with Saponin and Zirconium (TiO_2@Saponin/Zr(IV)), synthesized via a sol–gel method, to address this challenge, particularly in low salinity water injection scenarios. Characterization through FT-IR confirmed successful functionalization, indicated by the Zr–O band at 480 cm^{-1} and saponin bands around 1030–1085 cm^{-1} and 2919–2850 cm^{-1}. Zeta potential measurements showed that in low salinity brine, quartz and kaolinite exhibited highly negative potentials of − 32 mV and − 45 mV, respectively, while TiO_2@Saponin/Zr(IV) displayed a positive potential of + 19 mV. Importantly, mixtures of quartz and kaolinite with TiO_2@Saponin/Zr(IV) in low salinity conditions resulted in moderated zeta potentials of + 3 mV and − 2 mV, indicating surface charge modulation. Core flooding experiments further validated the composite's effectiveness. Injecting high salinity water resulted in a minor permeability reduction from 90 to 78 mD, while low salinity water injection caused a drastic drop from 90 to 8 mD. However, with the introduction of 0.5 wt% TiO_2@Saponin/Zr(IV) in low salinity water, the permeability reduction was significantly controlled, decreasing from 90 to 85 mD. These quantitative results demonstrate that TiO_2@Saponin/Zr(IV) effectively mitigates fines migration by modifying surface charge and preserving permeability, offering a promising solution for formation damage control and enhanced oil recovery.

Keywords Titania nanoparticles, Fines migration, Zeta potential, Enhanced oil recovery, Low salinity brine

[1]School of Mechanical and Electrical Engineering, GongQing Institute of Science and Technology, Jiujiang 332020, Jiangxi, China. [2]Department of Chemistry, University College of Duba, University of Tabuk, Tabuk, Saudi Arabia. [3]Department of Mechanical Engineering, Faculty of Engineering and Technology, Marwadi University Research Center, Marwadi University, Rajkot, Gujarat 360003, India. [4]Department of Mechanical Engineering, School of Engineering and Technology, JAIN (Deemed to be University), Bangalore, Karnataka, India. [5]Centre for Research Impact and Outcome, Chitkara University Institute of Engineering and Technology, Chitkara University, Rajpura, Punjab 140401, India. [6]Department of Mechanical Engineering, Sathyabama Institute of Science and Technology, Chennai, Tamil Nadu, India. [7]Department of Mechanical Engineering, Siksha 'O' Anusandhan (Deemed to be University), Bhubaneswar, Odisha 751030, India. [8]Department of Mechanical Engineering, Graphic Era Hill University, Dehradun, Uttarakhand 248002, India. [9]Department of Mechanical Engineering, Graphic Era Deemed to be University, Dehradun, Uttarakhand 248002, India. [10]Building and Construction Technical Engineering Department, College of Technical Engineering, The Islamic University, Najaf, Iraq. [11]Department of Computers Techniques Engineering, College of Technical Engineering, The Islamic University of Al Diwaniyah, Al Diwaniyah, Iraq. [12]Department of Computers Techniques Engineering, College of Technical Engineering, The Islamic University of Babylon, Babylon, Iraq. [13]Department of Mathematics and Information Technologies, Tashkent State Pedagogical University, Bunyodkor Avenue, 27, 100070 Tashkent, Uzbekistan. [14]Faculty of Engineering, Nangarhar University, Nangarhar, Afghanistan. [15]Department of Basic Medical Sciences, College of Applied Medical Science, King Khalid University, 61421 Abha, Saudi Arabia. ✉email: lym82775@sohu.com; samimsherzod@gmail.com

The increasing global demand for oil and the natural depletion of conventional oil reservoirs have driven the industry to adopt enhanced oil recovery (EOR) methods to maximize hydrocarbon production[1–7]. However, EOR techniques often disturb the delicate balance within reservoir systems, leading to the migration of fine particles, which can severely disrupt oil recovery efforts[8–12]. Fine migration can clog pore throats, reduce permeability, and compromise reservoir injectivity[13]. Among the causes of fine migration, Russell Thomas et al.[14] emphasized that kaolinite clay plays a significant role. Kaolinite, a layered silicate clay mineral, readily detaches from rock surfaces due to its weak Van der Waals interlayer forces and surface-charge interactions. During reservoir operations, changes in pH, ionic strength, or salinity can desorb kaolinite particles, causing them to migrate and block the flow paths of fluids. Temperature further exacerbates this problem; studies by Wang et al.[15] showed that elevated temperatures increase the propensity for fine migration by disrupting surface forces that anchor particles and increasing the kinetic energy of these fine particles, contributing to their mobilization.

Additionally, fine migration adversely impacts reservoir injectivity, as demonstrated by Russell Thomas in 2018[16], by building up around injection points and reducing fluid flow through critical zones. The phenomenon is further accentuated during low-salinity water flooding (LSWF), where clays destabilize fluid–solid interactions, leading to particle detachment, as noted by Tor Austad[1,17]. Recent advances by Aghdam et al.[18] have modeled interparticle forces using the DLVO (Derjaguin-Landau-Verwey-Overbeek) theory to predict the conditions under which fine migration occurs. Their work highlights how combining van der Waals attractions and electrostatic repulsions is key in regulating particle stability and movement within the reservoir[19–22].

To mitigate fine migration, researchers have explored the application of nanoparticles (NPs), which have shown promise in stabilizing reservoir conditions and minimizing the mobilization of fines[23–27]. Due to their high surface area and tunable surface properties, Nanoparticles interact with fine particles and the reservoir matrix to suppress migration. Various nanoparticles, such as silica (SiO_2), titanium dioxide (TiO_2), and iron oxide (Fe_3O_4), have been extensively studied in this area[28–32]. These particles can either adsorb onto the surface of fines to stabilize their position or modify the wettability of the reservoir rock to improve particle retention. For instance, silica nanoparticles are known for their ability to form an adhesive film-like layer that pins fines to the rock surface[33–36]. Similarly, TiO_2 nanoparticles, due to their surface reactivity and adsorption capacity[37–41], inhibit fine migration to a certain extent. Furthermore, nanoparticles can alter the electrostatic conditions within the reservoir by reducing repulsive forces between fines and reservoir rocks, thus lowering the potential for detachment[18,42–45]. Despite their effectiveness, however, the retention of nanoparticles within the reservoir can be challenging, alongside concerns regarding cost and long-term stability[46–49].

Surfactants have also gained attention as potential agents for controlling fine migration due to their ability to modify the surface charge and interfacial properties of fines and rock surfaces[28,50–52]. Surfactants such as saponins demonstrate an effective means of fine control by altering the surface charge, thereby suppressing particle detachment. Aghdam et al.[11,53] reported that saponins can modulate surface interactions by rebalancing the electrostatic forces that drive particle–matrix disruption. Additionally, researchers have examined the role of TiO_2 surfaces coated with surfactants, which show partial success in mitigating fine migration[54,55]. The surfactants reduce particle attachment to pore throats and modify the reservoir system's wettability, favoring fluid flow[28,56]. However, despite the encouraging results from combining nanoparticles and surfactants, no single material has yet been identified that eliminates fine migration. Most approaches still face challenges such as incomplete coverage, compatibility issues with reservoir brine, and adverse effects on overall reservoir flow properties. These limitations highlight the need for further exploration and development of advanced materials or synergistic formulations to restrain fine migration effectively.

The primary aim of this project is to develop a novel material to combat fines migration, a significant issue in subsurface reservoirs, especially during enhanced oil recovery. The research workflow begins with synthesizing titanium dioxide (TiO_2) nanoparticles using the sol–gel method. These nanoparticles are then functionalized in a two-step process, first by coating with saponin and subsequently incorporating Zirconium(IV) to create the TiO_2@Saponin/Zr(IV) composite. The synthesized materials, including TiO_2, TiO_2@Saponin, and TiO_2@Saponin/Zr(IV), are characterized using FT-IR spectroscopy to confirm the successful functionalization. To evaluate the effectiveness of TiO_2@Saponin/Zr(IV) in mitigating fines migration, zeta potential experiments are conducted on quartz, kaolinite, and TiO_2@Saponin/Zr(IV) particles, both individually and in mixtures, under high and low salinity brine conditions. Finally, core flooding tests are performed using three core samples. Core 1 is flooded with high salinity water, Core 2 with low salinity water, and Core 3 with low salinity water containing 0.5 wt% TiO_2@Saponin/Zr(IV). Permeability reduction is measured in each core to assess the impact of salinity and the composite additive on fine migration and formation damage.

Experimental section

Materials

Titanium isopropoxide

Titanium isopropoxide ($Ti[OCH(CH_3)_2]_4$) is a metal–organic compound commonly employed as a precursor in the synthesis of titanium dioxide (TiO_2) nanoparticles due to its high reactivity and ease of hydrolysis[57–59]. With a chemical purity exceeding 98%, this compound was procured from Merck, ensuring high-quality standards suitable for precision applications. At ambient conditions, titanium isopropoxide is a clear, colorless liquid with a characteristic odor. Its volatile and moisture-sensitive nature makes it an ideal reagent in the controlled synthesis of TiO_2 nanoparticles, offering advantages in achieving uniform particle size and phase purity.

Clay particles

Kaolinite, sourced from Pars Ore Company, is a key mineral found in clay-rich sandstone oil reservoirs, significantly affecting lubrication and fluid movement due to its crystalline structure and water absorption capacity. As a tectosilicate mineral, it has strong, compact bonds that resist fluid flow. Under low-salinity

Minerals composition	Mass%	Chemical composition	Mass%
Quartz	95	SiO_2	98.5
Kaolinite	3.2	Al_2O_3	1.1
Chlorite	1	Fe_2O_3	0.3
illite	0.5	MgO	0.06
Anorthite	0.3	TiO_2	0.04

Table 1. Mineral and chemical structure of core plugs acquired from XRD and XRF.

No	Length (cm)	Diameter (cm)	Porosity (Vol%)	Permeability (md)
1	10	3.81	21.5	85
2	10	3.81	22.4	83
3	10	3.81	221.9	84

Table 2. Features of cores used in this study.

water injection, the interactions between kaolinite particles and the surrounding fluid can change, potentially reducing particle adhesion, altering wetting conditions, and promoting the migration of fine particles within the sandstone[1,60,61].

Sand particles

Quartz (SiO_2) is a highly abundant and chemically stable tectonic mineral commonly present in petroleum deposits and sandstone formations, making it crucial in geological and petroleum engineering applications. This study used quartz with 99% purity as a reference material in batch experiments due to its exceptional stability and resistance to wear and environmental changes. These properties make quartz durable in oil formations and invaluable for conducting precise experiments to study the effects of various factors with reliable results[62–64].

Saponin

Saponin, a natural surfactant with a complex glycoside structure composed of a hydrophobic triterpenoid or steroid aglycone backbone and hydrophilic sugar moieties, exhibits excellent surface-active properties. With a purity greater than 95%, the saponin used in this study was purchased from Sigma Aldrich, ensuring high-quality standards suitable for experimental applications. Due to their emulsifying, foaming, and detergent-like capabilities, saponins are widely used in various fields, including pharmaceuticals, cosmetics, food industries, and research. Their unique amphiphilic structure makes them particularly effective in stabilizing emulsions and enhancing the bioavailability of compounds[65,66].

Zirconyl chloride

Zirconyl chloride octahydrate ($ZrOCl_20.8H_2O$) is an inorganic compound commonly used as a precursor in synthesizing zirconium-based materials due to its high solubility in water and extensive reactivity. This compound is characterized by the zirconium atom being coordinated with chloride ions and water molecules, forming a stable, hydrated salt. It is often utilized in various applications, including ceramics, catalysis, and polymerization processes, owing to its ability to introduce zirconium ions into different matrices efficiently. Additionally, $ZrOCl_20.8H_2O$ is instrumental in producing advanced materials such as zirconia (ZrO_2) due to its favorable chemical properties and easy handling during preparation stages[67,68].

Core plugs

Core plugs containing 3.2% by weight kaolinite were utilized in this study for core flooding experiments, designed to mimic natural conditions in sandstone oil reservoirs. X-ray Diffraction (XRD) and X-ray Fluorescence (XRF) analyses confirmed that kaolinite accounts for 5% by weight and is significantly present within the sample structures. The results of these analyses are detailed in Table 1.

The flooding of three core plug samples was utilized to examine the effect of the novel nanocomposite on the migration of fine particles in clay-rich sandstones, as detailed in Table 2. These investigations accurately evaluate kaolinite's influence on fluid dynamics and oil recovery techniques.

Experiments

Synthesizing TiO2@Saponin/Zr(IV)

Titanium dioxide (TiO_2) nanoparticles were synthesized via a sol–gel method using titanium isopropoxide (TTIP) as the precursor[69,70]. TTIP (10 mmol, 2.84 mL) was added dropwise into 100 mL of deionized water under constant stirring at 25 °C. The pH was maintained at 8 using an ammonia solution (7.5 mL). Stirring continued for 1 h at ambient temperature, and the suspension was subsequently heated to 80 °C for another hour to ensure complete hydrolysis. The resulting white precipitate, TiO_2 nanoparticles, was separated using centrifugation, washed several times with deionized water, and dried under vacuum at 60 °C.

A mixture of the obtained TiO_2 nanoparticles (1.5 g) and Saponin (2.5 g) was stirred in 30 ml of ethanol for 20 min at 25 °C to allow the saponin to coat the TiO_2 nanoparticles. After the reaction, the precipitate was collected, washed with ethanol, and dried at room temperature. The total yield was 3.92 g.

The TiO_2-coated saponin composite (0.3 g) and $ZrOCl_2 \cdot 8H_2O$ (0.43 g) were added to ethanol (10 mL) under stirring for 30 min at 25 °C. After stirring, the solvent was evaporated under ambient temperature to obtain the desired TiO_2@Saponin/Zr(IV) composite. The final product was washed thoroughly with ethanol, dried at room temperature, and prepared for subsequent characterization.

Zeta potential measurement

TiO2@Saponin/Zr(IV), Quartz, and kaolinite particles were ground into micro sizes to study their behavior in different salinity conditions. Two water samples with contrasting salinity levels were prepared: one with high salinity (250,000 mg/L) and the other with low salinity (1,000 mg/L). The objective was to assess how salinity influences the zeta potential of these particles, which indicates their surface charge and interaction with the surrounding environment. The particles were suspended in the two water samples, thoroughly mixed, and analyzed using a zeta-electrophoresis apparatus. This process measured the zeta potential by observing the motion of particles under an electric field, revealing their surface charge characteristics.

Additionally, particle size and distribution were analyzed using Dynamic Light Scattering (DLS), which measures the scattering pattern of light by suspended particles. Through this experiment, the researchers obtained insights into the interaction of quartz and kaolinite particles under varying salinity conditions. These findings contribute to understanding particle behavior in complex environments, such as oil extraction processes, where the interplay of surface charge, particle size, and salinity significantly impacts efficiency.

Core flooding test

The primary experiment undertaken in this study involved core flooding, conducted using the Vinci apparatus, as illustrated in Fig. 1. The experiment aimed to investigate the phenomenon of fine migration within sandstone oil reservoirs containing clay minerals. For this purpose, core plug samples with 3.2 wt% kaolinite content were utilized, comprising a mixture of quartz and kaolinite. These samples were meticulously prepared and placed in the core holder of the Vinci apparatus, where pressure and temperature parameters were carefully adjusted to replicate reservoir conditions. Following this preparation, a fluid of predetermined composition was steadily injected at 0.1 mL/min (1 ft/day) into the core samples to assess its influence on fine particle migration within the formation.

During the experiment, the pressure drop along the length of the core samples was continuously monitored, while the fluid output was systematically collected for detailed analysis[71,72]. The output fluid was examined to determine its composition, particle density, and chemical alterations caused by the injection process. The data was then analyzed rigorously to evaluate fluid behaviors, particle interactions, and flow characteristics under varying salinity and pressure conditions. The results from the core flooding experiment provide valuable insights into the complex interactions between fluids and minerals in petroleum reservoirs, particularly highlighting the fine migration phenomenon. These findings are vital for enhancing sandstone formations' oil extraction techniques and resource management strategies.

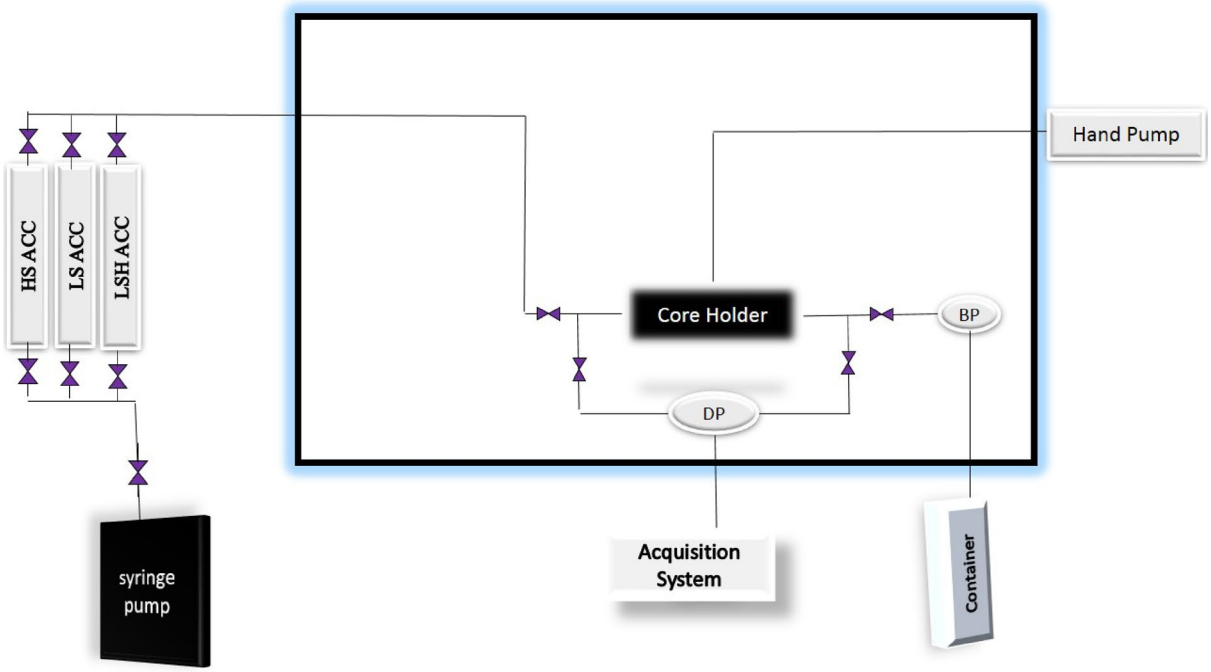

Fig. 1. The schematic of the Vinci device utilized for core flooding experiments.

All core flooding experiments were conducted at a temperature of 80 °C and a back pressure of 2000 psi to replicate reservoir conditions.

Results and discussion

TiO2@Saponin/Zr(IV) synthesize

The FT-IR analysis of (A) TiO_2 nanoparticles, (B) TiO_2@Saponin, and (C) TiO_2@Saponin/Zr(IV) is depicted in Fig. 2. Regarding Fig. 2A, The FT-IR spectra exhibit a peak at 450 cm^{-1}, which is attributed to the Ti–O stretching vibration[73,74]. A broad absorption band ranging from 3200 to 3400 cm^{-1} corresponds to O–H stretching vibrations[75,76]. This indicates the presence of hydroxyl groups (–OH) on the TiO_2 nanoparticle surface. New characteristic bands confirm the coating of TiO_2 with saponin (Fig. 2B). Peaks at 1030–1085 cm^{-1} correspond to C–O stretching vibrations[77], while the band at 1615 cm^{-1} denotes H–O–H bending vibrations[77] due to water molecules. The 2919 and 2850 cm^{-1} absorption corresponds to C–H stretching vibrations[78]. Furthermore, the broadband around 3380 cm^{-1} corresponds to hydroxyl (–OH) stretching vibrations[79], indicating the successful interaction of saponin with the TiO_2 nanoparticles. The FT-IR spectrum for TiO_2@Saponin/Zr(IV) (Fig. 2B) shows characteristic changes. A new band appears around 480 cm^{-1}, which is attributed to Zr–O bending vibrations. Additionally, the band at 450 cm^{-1} associated with Ti–O shifts slightly due to the presence of Zr–saponin bonds, demonstrating the successful incorporation of Zr(IV). The band at 1610 cm^{-1} corresponds to H–O–H bending vibrations, while bands around 3350 cm^{-1} illustrate –OH stretching vibrations. As compared to TiO_2@Saponin, the incorporation of Zr(IV) shifts the Ti–O stretching vibration to a slightly lower region (from 450 to ~ 480 cm^{-1}), confirming the successful interaction between Zr and the saponin-coated TiO_2 nanoparticles.

Additionally, transmission electron microscopy (TEM) was performed on the dry, synthesized TiO_2@Saponin/Zr(IV) nanocomposite. The TEM images (Fig. 3) confirm that the nanocomposites have an average particle size of approximately 33 nm. This nanoscale dimension is considerably smaller than both the typical pore throat sizes in sandstone cores and the average size of fines (e.g., kaolinite and quartz). Thus, the possibility of mechanical pore plugging by nanoparticles is minimal, supporting the suitability of the nanocomposite formulation for core flooding applications.

Brines

This section provides a comprehensive overview of the experimental results and discusses the indicators and outcomes of general mutations. Table 3 displays the composition of brines and water samples used in the zeta potential and core flooding experiments.

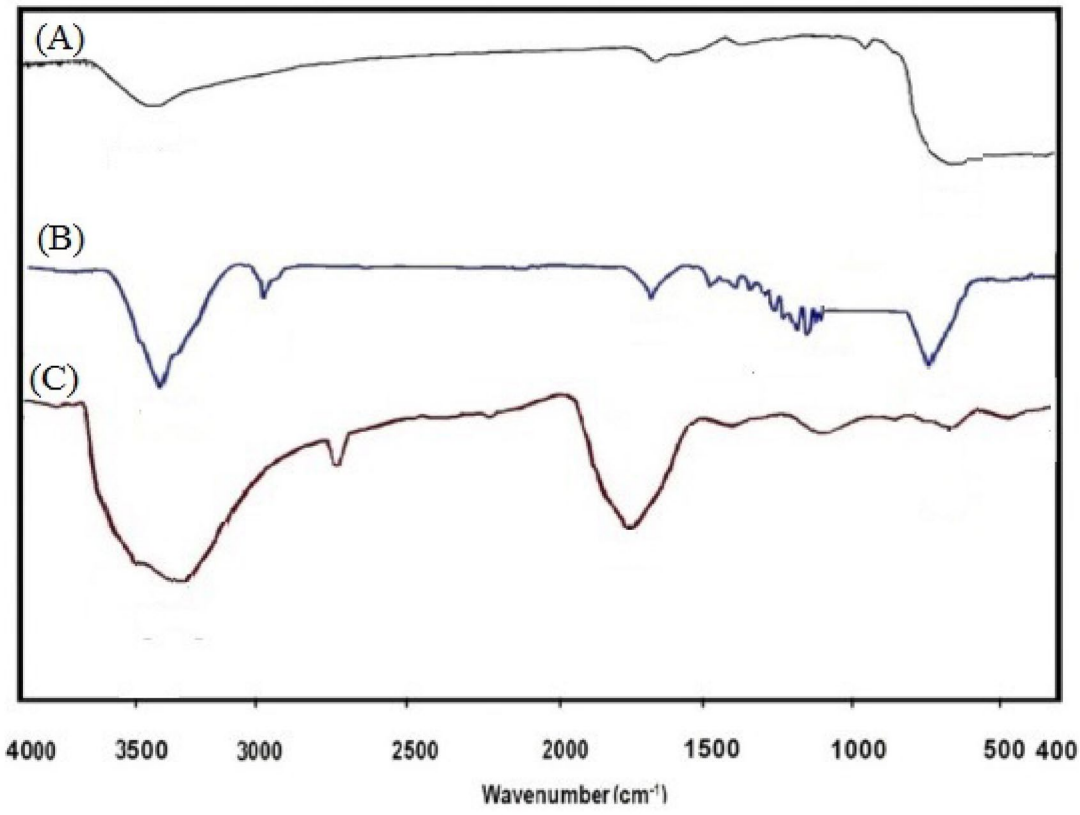

Fig. 2. FT-IR analysis of synthesized TiO_2@Saponin/Zr(IV).

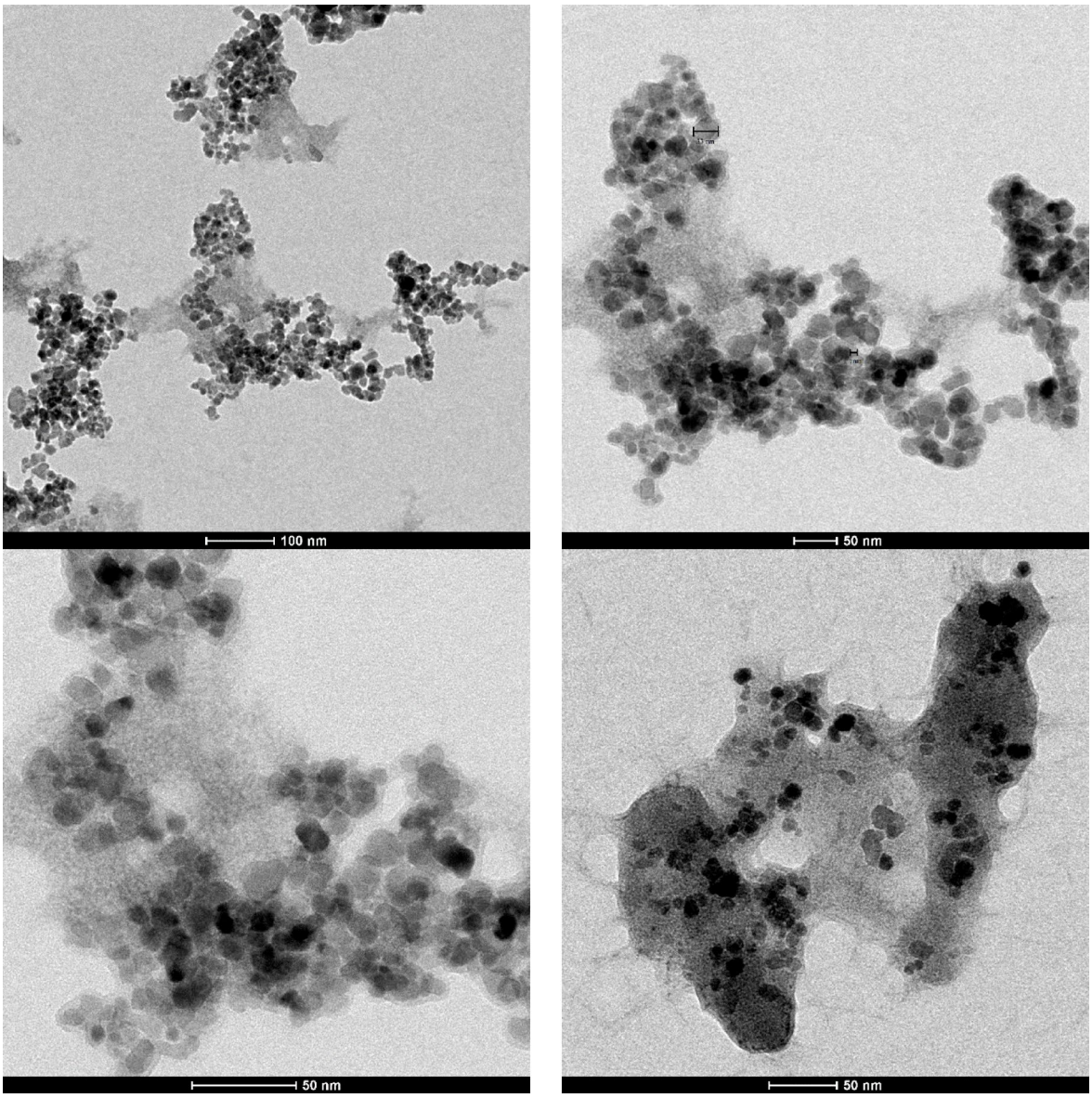

Fig. 3. TEM images related to the synthesized TiO_2@Saponin/Zr(IV).

Water sample	TiO2@Saponin/Zr(IV) (wt%)	NaCl (mg/L)	$CaCl_2$ (mg/L)	$MgCl_2$ (mg/L)	TDS (mg/L)
High salinity	0	150,000	60,000	40,000	250,000
Low salinity	0	600	250	150	1000

Table 3. Water samples related to this research.

Zeta potential test

The zeta potential measurements in Table 4 reveal significant differences in surface charge behavior for quartz, kaolinite, and TiO_2@Saponin/Zr(IV) particles in brine with varying salinity levels. In high salinity water, the zeta potentials for quartz, kaolinite, and TiO_2@Saponin/Zr(IV) are approximately 0 mV, − 2 mV, and + 1 mV, respectively. These low magnitudes indicate surface charge compensation due to the presence of high concentrations of ions in the saline environment[80,81]. In highly saline water, the electrical double layer surrounding the particles is compressed, reducing electrostatic interactions and effectively neutralizing the surface charge. The ions in high salinity water adsorb onto the particle surfaces, counteracting their inherent negative or positive charges and leading to minimal repulsion or attraction between particles. This charge compensation highlights the role of ionic strength in suppressing fine detachment and particle migration under high salinity conditions.

Particle type	High salinity	Low salinity
Quartz (1 wt%)	0	− 32
Kaolinite (1 wt%)	− 2	− 45
TiO2@Saponin/Zr(IV) (1 wt%)	+ 1	+ 19
Quartz (0.5 wt%) + TiO_2@Saponin/Zr(IV) (0.5 wt%)	0	+ 3
Kaolinite (0.5 wt%) + TiO_2@Saponin/Zr(IV) (0.5 wt%)	0	− 2

Table 4. Zeta potential values (mv) obtained for various particles in different brine solutions.

In contrast, in low salinity water, the zeta potentials for quartz, kaolinite, and TiO_2@Saponin/Zr(IV) are − 32 mV, − 45 mV, and + 19 mV, respectively. These measurements illustrate a considerable increase in surface charge magnitude for all particles. In low salinity conditions, the electrical double layer surrounding the particles is significantly expanded due to the reduced ionic strength of the medium. This results in unshielded surface charges, enhanced electrostatic repulsion between negatively charged quartz and kaolinite particles, and increased stabilization of particle suspensions. The strong negative charges observed for quartz and kaolinite suggest a high potential for particle detachment and migration in low salinity environments, as mutual repulsion overcomes the forces holding fine particles attached to the substrate. This phenomenon is particularly relevant in petroleum reservoirs, as particle detachment can lead to fine migration, negatively affecting production efficiency by clogging pore spaces and altering permeability.

Introducing TiO_2@Saponin/Zr(IV) into the low-salinity brine significantly alters the zeta potential and interaction between quartz and kaolinite particles. Table 4 shows that the zeta potential of the quartz-TiO_2@Saponin/Zr(IV) mixture increases to + 3 mV, while the kaolinite-TiO_2@Saponin/Zr(IV) mixture has a zeta potential of − 2 mV. This shift in zeta potential suggests that TiO2@Saponin/Zr(IV) can modify the overall charge of the system through complex interfacial interactions. The positive potential on quartz when mixed with TiO_2@Saponin/Zr(IV) may originate from the successful adsorption of positively charged Zr(IV), while the negative potential on kaolinite could reflect the combined influence of saponin functional groups and kaolinite's surface structure[82,83]. This change in surface charge reduces repulsive forces between the particles and promotes attraction, effectively preventing fine particle detachment and migration. The ability of TiO_2@Saponin/Zr(IV) to mediate particle interactions highlights its potential as an additive to control fine migration in enhanced oil recovery operations.

Chemically, the observed behavior is strongly tied to the interaction of ions and molecules within the fluid. In low-salinity brine, insufficient ionic coverage exposes the inherent surface charges of quartz and kaolinite, resulting in higher zeta potential magnitudes. However, adding TiO_2@Saponin/Zr(IV) introduces new electrostatic and chemical interactions. The Zr(IV) ions, being positively charged, can neutralize the negative charges on particle surfaces, while the saponin molecules may form hydrogen bonds or other polar interactions, stabilizing particle suspensions and minimizing detachment. These findings underscore TiO_2@Saponin/Zr(IV) 's role in mitigating the adverse effects of particle detachment and fine migration, providing a promising solution for enhanced oil recovery applications.

The zeta potential of particles is strongly influenced by the pH of the surrounding medium due to the ionization or adsorption of hydrogen ions (H^+) and hydroxyl ions (OH^-) on the particle surfaces. In this study, zeta potential measurements were conducted in high salinity brine (pH 5.5) and low salinity brine (pH 6.0), reflecting the typical conditions of injection brine during low salinity water flooding. At these pH levels, TiO_2@Saponin/Zr(IV) exhibited a positive zeta potential (+ 19 mV at pH 6.0), while quartz and kaolinite were highly negative (− 32 mV and − 45 mV) under low salinity conditions. A decrease in pH (more acidic conditions) would further increase the zeta potential of the TiO_2@Saponin/Zr(IV) composite due to protonation of the hydroxyl and other functional groups on its surface, enhancing its positive charge. This phenomenon occurs because at lower pH, an increased concentration of H^+ ions neutralizes any negative surface charge, shifting the zeta potential positively. Conversely, in strongly basic environments, deprotonation effects dominate, leading to reduced or even negative zeta potentials. This behavior demonstrates the resilience of the TiO_2@Saponin/Zr(IV) composite in moderately acidic conditions, as it maintains a sufficiently positive surface charge capable of modulating the electrostatic interaction between fines and rock surfaces, thereby continuing to mitigate fines migration effectively. Future studies could explore the robustness of this material's zeta potential across a broader pH range to evaluate its performance in reservoirs with varying pH conditions.

Core flooding

Core flooding experiments provide valuable insights into the effects of salinity and engineered nanoparticles such as TiO_2@Saponin/Zr(IV) on clay-rich sandstone formations. These experiments focus on fine migration phenomena, permeability reduction, and the mitigation of formation damage. The results indicate that the interplay between surface charge (zeta potential) and brine composition determines the behavior of fine particles during brine injection. Below, a scientific discussion is offered based on the results.

As depicted in Fig. 4, when high salinity water was injected, the permeability of the clay-rich core decreased minimally, from 90 to 78 mD. This minor reduction can be attributed to the limited detachment and migration of fine particles such as kaolinite and quartz. The zeta potential data provide a clear justification for this observation. Under high salinity conditions, the zeta potential of kaolinite particles was measured as -2 mV, while quartz particles exhibited a 0 mV surface charge. This reflects a significant reduction in the magnitude of negative surface charge compared to low salinity conditions. The high ionic strength of the brine compresses the

electrical double layer surrounding the particles, suppressing electrostatic repulsion between them and reducing the likelihood of particle detachment. Additionally, the near-neutral zeta potentials of quartz and kaolinite under HSW conditions stabilize these particles, preventing migration. The core flooding experiments were conducted under controlled reservoir-like conditions with a temperature of 80°C and a back pressure of 2000 psi. These parameters closely mimic the thermal and pressure environments of typical sandstone reservoirs, ensuring that the experimental results are representative of real-field conditions and applicable for predicting fines migration behavior.

In the second experiment, low salinity water was injected into core 2, which resulted in a dramatic permeability reduction from 90 to 8 md within only 5 pore volumes, as depicted in Fig. 5. This significant decrease in permeability is intimately linked to the chemical dynamics of the particles when subjected to a low ionic strength environment. According to the zeta potential data, low salinity conditions render quartz and kaolinite surfaces significantly more negative; quartz exhibits a zeta potential of -32 mV and kaolinite -45 mV. The increase in the magnitude of the opposing surface potential indicates an extended electrical double layer that develops without sufficient ionic screening. Although a more negative zeta potential typically implies a stronger repulsion among dispersed particles, it destabilizes the fines usually attached to the rock surface. The increased repulsive forces facilitate the detachment of fine particles under the shear forces imposed by fluid injection. Once mobilized, these fines may migrate and eventually deposit in narrower pore constrictions further downstream, clogging pore throats and leading to a significant drop in permeability. This observation underscores the delicate balance between repulsive interparticle forces and the hydrodynamic forces of the flooding process; under low salinity conditions, these forces combine to trigger severe formation damage through fines migration and deposition.

The third experiment, which is depicted in Fig. 6, introduces a low-salinity water system that is amended with 0.5 wt% TiO_2@Saponin/Zr(IV) and injected into core 3. The resulting permeability reduction is much more controlled, decreasing only from 90 to 85 md. The zeta potential measurements of the TiO_2@Saponin/Zr(IV) composite clarify the chemistry behind this mitigation strategy. The TiO_2@Saponin/Zr(IV) particles display a positive zeta potential of + 19 mV in low salinity conditions. When these additives interact with quartz and kaolinite fines, the overall particle suspensions show moderated zeta potentials; for example, mixtures of quartz with the composite yield a near-neutral value of + 3 mV, while kaolinite combined with the composite is adjusted to approximately − 2 mV. Shifting toward a neutral potential is crucial because surfaces with little net charge do not experience the extreme repulsive interactions observed in low salinity conditions without the additive. The TiO_2@Saponin/Zr(IV) nanoparticles function as an electrostatic buffer that mitigates excessive charge repulsion, reducing the likelihood of fine detachment and migration. The slight permeability reduction observed in this core indicates a stabilization mechanism in which the additive alters the surface chemistry of detaching particles to encourage adhesion to the rock surface rather than uncontrolled dispersion. This chemical stabilization minimizes pore throat blockage and formation damage even under otherwise aggressive conditions where low salinity would promote substantial fines migration. It is important to note that the mechanism by which TiO_2@Saponin/Zr(IV) nanocomposites stabilize fines and maintain permeability does not primarily involve direct pore blocking or physical filtration, as evidenced by their small size. TEM analysis demonstrates that the average diameter of these nanoparticles is ~ 33 nm, significantly smaller than the average fines size and much smaller than typical pore throat sizes within reservoir sandstone. Therefore, the nanocomposites act through modulation of surface charge and electrostatic stabilization, rather than acting as mechanical barriers to

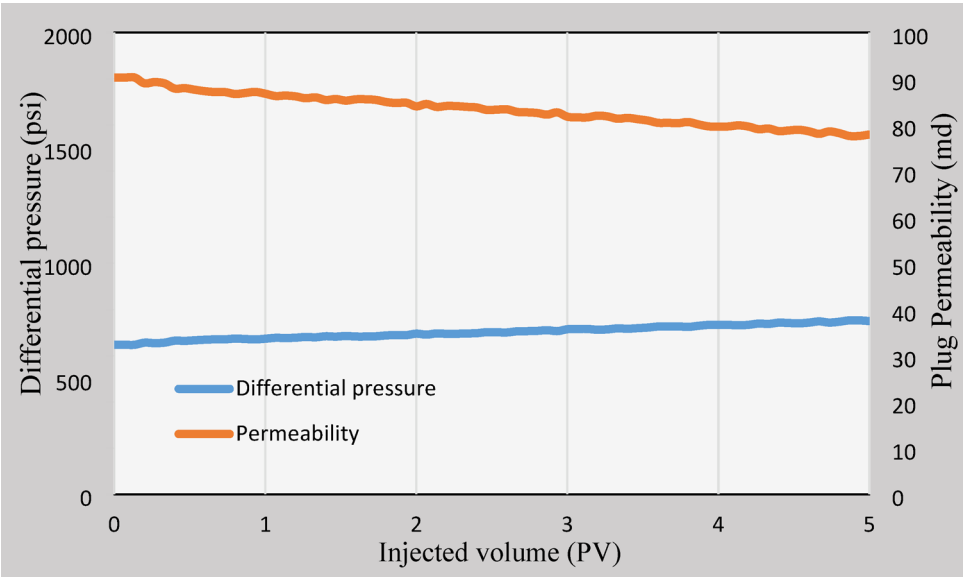

Fig. 4. Core flooding experiment results obtained from high salinity water injection into core 1 at 80 °C and at a back pressure of 2000 psi.

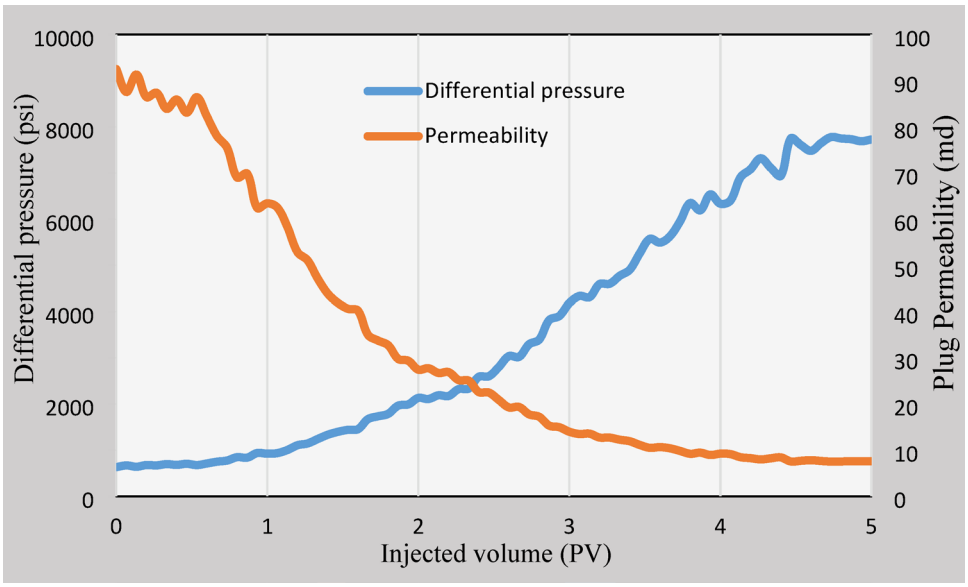

Fig. 5. Core flooding experiment results obtained from low salinity water injection into core 2 at 80 °C and at a back pressure of 2000 psi.

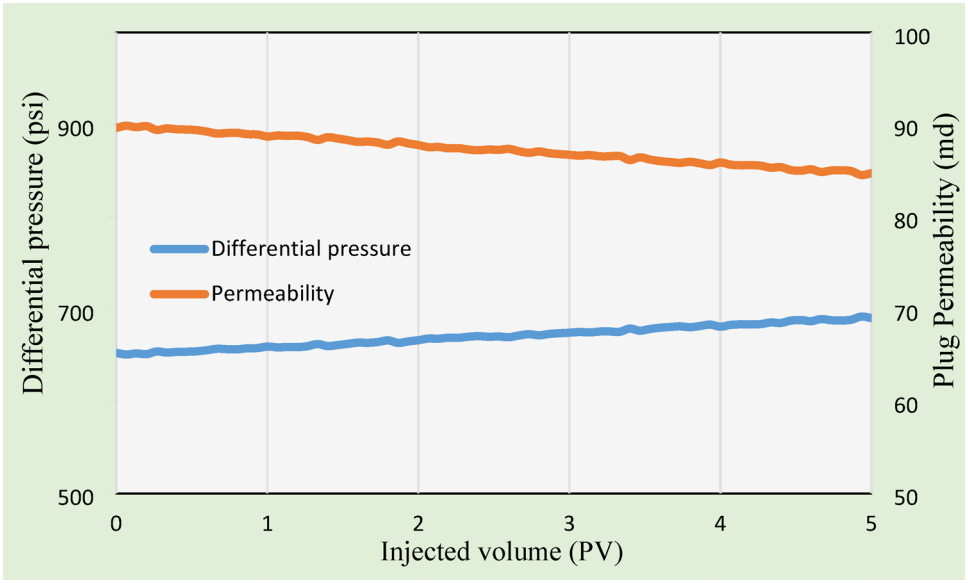

Fig. 6. Core flooding experiment results obtained from low salinity water injection containing TiO_2@Saponin/Zr(IV) nanoparticles into core 3 at 80 °C and at a back pressure of 1000 psi.

flow. This distinction reinforces the chemical, rather than physical, basis for improved permeability observed in the presence of the nanocomposite, validating the proposed fines migration control mechanism.

In summary, these core flooding experiments demonstrate that the chemical environment, particularly the ionic strength of the injected brine and the associated zeta potential values of rock mineral constituents, plays a critical role in fine migration and formation damage. High salinity water compresses the double layer, thereby maintaining fines in place, whereas low salinity water expands the double layer, resulting in vigorous fine detachment and migration. This phenomenon is clearly reflected in quartz and kaolinite's highly negative zeta potentials in such conditions. Additionally, including TiO_2@Saponin/Zr(IV) in the low salinity system effectively modifies the surface charge environment by shifting the zeta potential toward less disruptive values, which preserves a higher permeability. This detailed interplay between surface chemistry and fluid composition highlights the potential of additive-assisted flooding strategies to control formation damage in clay-rich sandstones. The zeta potential measurements serve as a fundamental link that bridges the microscopic chemical

No	Fluid	Initial permeability (md)	Final permeability (md)
1	High salinity	90	78
2	Low salinity	90	8
3	Low salinity containing TiO2@Saponin/Zr(IV) 0.5 wt%	90	85

Table 5. Summary of core flooding experiment acquired data.

forces with the macroscopic flow behavior observed in these experiments. A summary of core flooding data is presented in Table 5.

Mechanism of action of TiO_2@Saponin/Zr(IV) in reducing fine migration
The TiO_2@Saponin/Zr(IV) composite reduces fines migration by stabilizing particle suspensions and adjusting surface chemistry. As a natural surfactant, Saponin increases surface hydrophilicity and provides functional groups for adequate bonding. Zirconium ions (Zr(IV)), incorporated into the composite, impart a positive charge, neutralizing the negative charges of quartz and kaolinite fines in low salinity environments. This electrostatic buffering reduces repulsive forces between particles, minimizing fine detachment and promoting adhesion to rock surfaces. Additionally, hydrogen bonding and polar interactions mediated by saponin reinforce particle stability, preventing uncontrolled migration through pore spaces. This synergistic mechanism maintains fluid permeability by counteracting the destabilizing effects of substantial electrical double-layer expansion in low-salinity brine injection.

Industrial implications
This research introduces a novel strategy to mitigate formation damage caused by fines migration in enhanced oil recovery applications, particularly during low salinity water injection. TiO_2@Saponin/Zr(IV) offers a cost-effective and scalable approach to improving reservoir productivity. The composite reduces operational risks such as injectivity decline and formation blockage by maintaining permeability and minimizing clogging. Its compatibility with existing brine injection methods and environmental safety (through saponin) further emphasize its feasibility for large-scale industrial use. This advancement provides oil and gas operators with a robust water flooding additive that enhances recovery rates while mitigating the adverse effects of fine detachment, contributing significantly to sustainable reservoir management.

It should be noted that the current study was designed specifically for water injection applications, where the principal challenge is injectivity decline due to fines migration during low salinity water injection. The composite's mechanism addresses fines stabilization and permeability preservation in fully water-saturated, clay-rich sandstones without the presence of a hydrocarbon phase. As such, interfacial tension reduction and wettability alteration were not investigated, nor do these factors play a critical role in the presented injectivity improvement mechanism under these experimental conditions. While the TiO_2@Saponin/Zr(IV) nanocomposite holds potential for broader reservoir applications, its effects on oil–water IFT and wettability would require separate, dedicated studies under multiphase flow conditions and should be considered in future research when targeting enhanced oil recovery in production wells.

Conclusion
In conclusion, this study successfully synthesized and characterized the TiO_2@Saponin/Zr(IV) composite, demonstrating its significant potential in mitigating fines migration and formation damage during enhanced oil recovery, particularly in low salinity scenarios. Zeta potential measurements revealed a shift from highly negative potentials for quartz (− 32 mV) and kaolinite (− 45 mV) in low salinity brine to near-neutral values (+ 3 mV and − 2 mV, respectively) when mixed with TiO_2@Saponin/Zr(IV), indicating effective surface charge modulation. Core flooding experiments quantitatively confirmed these findings. While high salinity water injection resulted in a minor permeability reduction of approximately 13% (from 90 to 78 mD), low salinity water injection caused a severe 91% reduction in permeability (from 90 to 8 mD). Introducing 0.5 wt% TiO_2@Saponin/Zr(IV) in low salinity water significantly limited permeability reduction to only about 5.5% (from 90 to 85 mD). These results underscore the efficacy of TiO_2@Saponin/Zr(IV) in stabilizing fines, maintaining permeability, and preventing drastic formation damage. The composite presents a promising, efficient, and potentially environmentally conscious additive for improving oil recovery and ensuring sustainable reservoir management by effectively addressing fines migration challenges in oilfield operations. This study is limited to water injection wells and does not address oil-phase mechanisms such as IFT reduction or wettability alteration. For future application in EOR contexts involving oil production wells, it is required to fully evaluate its impact on reservoir wettability and interfacial properties.

Data availability
Data will be available at the academic request from the corresponding author.

Received: 19 March 2025; Accepted: 20 May 2025
Published online: 29 May 2025

References

1. Puntervold, T. et al. Role of kaolinite clay minerals in enhanced oil recovery by low salinity water injection. *Energy Fuels* **32**(7), 7374–7382 (2018).
2. Sheng, J. J. Formation damage in chemical enhanced oil recovery processes. *Asia-Pac. J. Chem. Eng.* **11**(6), 826–835 (2016).
3. Najafi, S. A. S. et al. Experimental and theoretical investigation of CTAB microemulsion viscosity in the chemical enhanced oil recovery process. *J. Mol. Liq.* **232**, 382–389 (2017).
4. Hasankhani, G. M. et al. Experimental investigation of asphaltene-augmented gel polymer performance for water shut-off and enhancing oil recovery in fractured oil reservoirs. *J. Mol. Liq.* **275**, 654–666 (2019).
5. Hasankhani, G. M. et al. An experimental investigation of polyacrylamide and sulfonated polyacrylamides based gels crosslinked with cr(III)-acetate for water shutoff in fractured oil reservoirs. *J. Dispersion Sci. Technol.* **39**(12), 1780–1789 (2018).
6. Takassi, M. A. et al. The preparation of an amino acid-based surfactant and its potential application as an EOR agent. *Pet. Sci. Technol.* **35**(4), 385–391 (2017).
7. Khojastehmehr, M., Madani, M. & Daryasafar, A. Screening of enhanced oil recovery techniques for Iranian oil reservoirs using TOPSIS algorithm. *Energy Rep.* **5**, 529–544 (2019).
8. Maini, B., Wassmuth, F. & Schramm, L. L. Fines migration in petroleum reservoirs. In *Suspensions: Fundamentals and Applications in the Petroleum Industry* 321–375 (American Chemical Society, 1996).
9. Lemon, P., et al. Effects of injected water chemistry on waterflood sweep efficiency via induced fines migration. In *SPE International Symposium on Oilfield Chemistry*. (OnePetro, 2011).
10. Madani, M. et al. Fundamental investigation of an environmentally-friendly surfactant agent for chemical enhanced oil recovery. *Fuel* **238**, 186–197 (2019).
11. Khezerlooe-ye Aghdam, S. et al. Mechanistic assessment of Seidlitzia Rosmarinus-derived surfactant for restraining shale hydration: A comprehensive experimental investigation. *Chem. Eng. Res. Des.* **147**, 570–578 (2019).
12. Madani, M. et al. Modeling of CO_2-brine interfacial tension: Application to enhanced oil recovery. *Pet. Sci. Technol.* **35**(23), 2179–2186 (2017).
13. Deng, R., Dong, J. & Dang, L. Numerical simulation and evaluation of residual oil saturation in waterflooded reservoirs. *Fuel* **384**, 134018 (2025).
14. Russell, T. et al. Effects of kaolinite in rocks on fines migration. *J. Natl. Gas Sci. Eng.* **45**, 243–255 (2017).
15. Wang, Y. et al. Effect of temperature on mineral reactions and fines migration during low-salinity water injection into Berea sandstone. *J. Petrol. Sci. Eng.* **202**, 108482 (2021).
16. Russell, T. et al. Effects of delayed particle detachment on injectivity decline due to fines migration. *J. Hydrol.* **564**, 1099–1109 (2018).
17. Austad, T., RezaeiDoust, A. & Puntervold, T. Chemical Mechanism of Low Salinity Water Flooding in Sandstone Reservoirs. In *SPE Improved Oil Recovery Symposium* SPE-129767-MS (2010).
18. Khezerloo-yeAghdam, S., Kazemi, A. & Ahmadi, M. Theoretical and experimental study of fine migration during low-salinity water flooding: Effect of brine composition on interparticle forces. *SPE Reserv. Evaluat. Eng.* **26**(02), 228–243 (2023).
19. Austad, T. et al. Conditions for a low-salinity enhanced oil recovery (EOR) effect in carbonate oil reservoirs. *Energy Fuels* **26**(1), 569–575 (2012).
20. Shalabi, E. W. A., Sepehrnoori, K. & Delshad, M. Mechanisms behind low salinity water injection in carbonate reservoirs. *Fuel* **121**, 11–19 (2014).
21. Hua, L. et al. Semi-analytical study of pile-soil interaction on a permeable pipe pile subjected to rheological consolidation of clayey soils. *Int. J. Numer. Anal. Methods Geomech.* **49**(3), 1058–1074 (2025).
22. Cao, D. et al. Correction of linear fracture density and error analysis using underground borehole data. *J. Struct. Geol.* **184**, 105152 (2024).
23. Mansouri, M., Nakhaee, A. & Pourafshary, P. Effect of SiO_2 nanoparticles on fines stabilization during low salinity water flooding in sandstones. *J. Petrol. Sci. Eng.* **174**, 637–648 (2019).
24. Habibi, A. et al. Reduction of fines migration by nanofluids injection: An experimental study. *SPE J.* **18**(02), 309–318 (2012).
25. Yanchun, L. I. et al. Surrogate model for reservoir performance prediction with time-varying well control based on depth generative network. *Pet. Explor. Dev.* **51**(5), 1287–1300 (2024).
26. Zhu, B. et al. Micro-particle manipulation by single beam acoustic tweezers based on hydrothermal PZT thick film. *AIP Adv.* **6**(3), 48 (2016).
27. Zhu, B.-P. et al. Synthesis of Mg [Ti2] O4 by spark plasma sintering. *Mater. Lett.* **61**(2), 578–581 (2007).
28. Dordzie, G. & Dejam, M. Enhanced oil recovery from fractured carbonate reservoirs using nanoparticles with low salinity water and surfactant: A review on experimental and simulation studies. *Adv. Coll. Interface. Sci.* **293**, 102449 (2021).
29. Olayiwola, S. O. & Dejam, M. A comprehensive review on interaction of nanoparticles with low salinity water and surfactant for enhanced oil recovery in sandstone and carbonate reservoirs. *Fuel* **241**, 1045–1057 (2019).
30. Huang, T. & Clark, D. E. Enhancing oil recovery with specialized nanoparticles by controlling formation-fines migration at their sources in waterflooding reservoirs. *SPE J.* **20**(04), 743–746 (2015).
31. Ahmadi, M. et al. Zeta-potential investigation and experimental study of nanoparticles deposited on rock surface to reduce fines migration. *SPE J.* **18**(03), 534–544 (2013).
32. Zhu, B. et al. Lift-off PMN–PT thick film for high-frequency ultrasonic biomicroscopy. *J. Am. Ceram. Soc.* **93**(10), 2929–2931 (2010).
33. Wan, S. et al. An overview of inorganic polymer as potential lubricant additive for high temperature tribology. *Tribol. Int.* **102**, 620–635 (2016).
34. Erdemir, A. & Martin, J. M. Superior wear resistance of diamond and DLC coatings. *Curr. Opin. Solid State Mater. Sci.* **22**(6), 243–254 (2018).
35. Cao, H. et al. Hydrogels: A promising therapeutic platform for inflammatory skin diseases treatment. *J. Mater. Chem. B* **12**(33), 8007–8032 (2024).
36. Zhu, B. et al. New fabrication of high-frequency (100-MHz) ultrasound PZT film kerfless linear array [Correspondence]. *IEEE Trans. Ultrason. Ferroelectr. Freq. Control* **60**(4), 854–857 (2013).
37. Belessi, V. et al. Removal of reactive red 195 from aqueous solutions by adsorption on the surface of TiO_2 nanoparticles. *J. Hazard. Mater.* **170**(2–3), 836–844 (2009).
38. Giammar, D. E., Maus, C. J. & Xie, L. Effects of particle size and crystalline phase on lead adsorption to titanium dioxide nanoparticles. *Environ. Eng. Sci.* **24**(1), 85–95 (2007).
39. Zaki, M. I. et al. TiO_2 nanoparticle size dependence of porosity, adsorption and catalytic activity. *Colloids Surf. A* **385**(1–3), 195–200 (2011).
40. Gan, B. et al. Phase transitions of CH_4 hydrates in mud-bearing sediments with oceanic laminar distribution: Mechanical response and stabilization-type evolution. *Fuel* **380**, 133185 (2025).
41. Zhu, B. P. et al. Structure and electrical properties of (111)-oriented Pb (Mg 1/3 Nb 2/3)O_3-$PbZrO_3$-$PbTiO_3$ thin film for ultra-high-frequency transducer applications. *IEEE Trans. Ultrason. Ferroelectr. Freq. Control* **58**(9), 1962–1967 (2011).
42. Yang, Y. et al. Review on physical and chemical factors affecting fines migration in porous media. *Water Res.* **214**, 118172 (2022).
43. El-Monier, I. A. & Nasr-El-Din, H. A. *Mitigation of fines migration using a new clay stabilizer: a mechanistic study*. In *SPE European Formation Damage Conference* (2011).

44. Zhang, L. et al. Seepage characteristics of broken carbonaceous shale under cyclic loading and unloading conditions. *Energy Fuels* **38**(2), 1192–1203 (2023).
45. Zhang, L. et al. Seepage characteristics of coal under complex mining stress environment conditions. *Energy Fuels* **38**(17), 16371–16384 (2024).
46. Zhu, B. P. et al. *Sol-Gel Derived PMN-PT Thick Film for High Frequency Ultrasound Transducer Applications* (IEEE, 2009).
47. Wei, J. et al. (±)-Hypandrone A, a pair of polycyclic polyprenylated acylphloroglucinol enantiomers with a caged 7/6/5/6/6 pentacyclic skeleton from Hypericum androsaemum. *Org. Chem. Front.* **11**(12), 3459–3464 (2024).
48. Li, X., et al. Effect of different hydrogen donors on the catalytic conversion of levulinic acid to γ-valerolactone over non-noble metal catalysts. *J. Ind. Eng. Chem*. (2024).
49. Xu, J. et al. Study on fuel injection stability improvement in marine low-speed dual-fuel engines. *Appl. Therm. Eng.* **253**, 123729 (2024).
50. Yue, L. et al. Insights into mechanism of low salinity water flooding in sandstone reservoir from interfacial features of oil/brine/rock via intermolecular forces. *J. Mol. Liq.* **313**, 113435 (2020).
51. Tariq, Z. et al. Novel gemini surfactant as a clay stabilizing additive in fracturing fluids for unconventional tight sandstones: Mechanism and performance. *J. Petrol. Sci. Eng.* **195**, 107917 (2020).
52. Niu, Q. et al. Inversion and optimization of CO_2 + O_2 in situ leaching of blasting-stimulated sandstone-type uranium deposits. *Phys. Fluids* **37**(3), 54 (2025).
53. Aghdam, S.K.-Y., Kazemi, A. & Ahmadi, M. Studying the effect of various surfactants on the possibility and intensity of fine migration during low-salinity water flooding in clay-rich sandstones. *Results Eng.* **18**, 101149 (2023).
54. Madadizadeh, A., Sadeghein, A. & Riahi, S. The use of nanotechnology to prevent and mitigate fine migration: A comprehensive review. *Rev. Chem. Eng.* **38**(1), 1–16 (2022).
55. Cha, M.-H. et al. Proteomic identification of macrophage migration-inhibitory factor upon exposure to TiO_2 particles. *Mol. Cell. Proteom.* **6**(1), 56–63 (2007).
56. Huang, T., Crews, J. B. & Willingham, J. R. *Nanoparticles for Formation Fines Fixation and Improving Performance of Surfactant Structure Fluids* (European Association of Geoscientists & Engineers, 2008).
57. Mahshid, S., Askari, M. & Ghamsari, M. S. Synthesis of TiO_2 nanoparticles by hydrolysis and peptization of titanium isopropoxide solution. *J. Mater. Process. Technol.* **189**(1–3), 296–300 (2007).
58. Aarik, J. et al. Titanium isopropoxide as a precursor for atomic layer deposition: Characterization of titanium dioxide growth process. *Appl. Surf. Sci.* **161**(3–4), 385–395 (2000).
59. Ritala, M. et al. Titanium isopropoxide as a precursor in atomic layer epitaxy of titanium dioxide thin films. *Chem. Mater.* **5**(8), 1174–1181 (1993).
60. Miranda-Trevino, J. C. & Coles, C. A. Kaolinite properties, structure and influence of metal retention on pH. *Appl. Clay Sci.* **23**(1), 133–139 (2003).
61. Bish, D. L. Rietveld refinement of the kaolinite structure at 1.5 K. *Clays Clay Miner.* **41**(6), 738–744 (1993).
62. Worden, R. H. & Morad, S. Quartz cementation in oil field sandstones: A review of the key controversies. In *Quartz Cementation in Sandstones* 1–20 (2000).
63. Dong, T. et al. Quartz types and origins in the paleozoic Wufeng-Longmaxi Formations, Eastern Sichuan Basin, China: Implications for porosity preservation in shale reservoirs. *Mar. Pet. Geol.* **106**, 62–73 (2019).
64. Garcia, D. C. S., Wang, K. & Figueiredo, R. B. The influences of quartz content and water-to-binder ratio on the microstructure and hardness of autoclaved Portland cement pastes. *Cem. Concr. Compos.* **91**, 138–147 (2018).
65. Mitra, S. & Dungan, S. R. Micellar properties of *Quillaja saponin*. 1. Effects of temperature, salt, and pH on solution properties. *J. Agric. Food Chem.* **45**(5), 1587–1595 (1997).
66. Adenutsi, C. D. et al. Review on potential application of saponin-based natural surfactants for green chemical enhanced oil recovery: Perspectives and progresses. *Energy Fuels* **37**(13), 8781–8823 (2023).
67. Mak, T. C. W. Refinement of the crystal structure of zirconyl chloride octahydrate. *Can. J. Chem.* **46**(22), 3491–3497 (1968).
68. Wang, M.-L., Liu, B.-L. & Shih, Z.-W. Sol synthesis from zirconyl chloride octahydrate in NTA-ammonia solution. *J. Cryst. Growth* **183**(3), 398–408 (1998).
69. Sharma, A., Karn, R. K. & Pandiyan, S. K. Synthesis of TiO_2 nanoparticles by sol–gel method and their characterization. *J. Basic Appl. Eng. Res.* **1**(9), 1–5 (2014).
70. Šegota, S. et al. Synthesis, characterization and photocatalytic properties of sol–gel TiO_2 films. *Ceram. Int.* **37**(4), 1153–1160 (2011).
71. Kazemi, A., Khezerloo-ye Aghdam, S. & Ahmadi, M. Theoretical and experimental investigation of the impact of oil functional groups on the performance of smart water in clay-rich sandstones. *Sci. Rep.* **14**(1), 20172 (2024).
72. Khezerloo-ye Aghdam, S., Kazemi, A. & Ahmadi, M. Studying the effect of surfactant assisted low-salinity water flooding on clay-rich sandstones. *Petroleum* **10**(2), 306–318 (2024).
73. Scarano, D. et al. Fourier-transform infrared and Raman spectra of pure and Al-, B-, Ti- and Fe-substituted silicalites: Stretching-mode region. *J. Chem. Soc., Faraday Trans.* **89**(22), 4123–4130 (1993).
74. Astorino, E. et al. Spectroscopic characterization of silicalite-1 and titanium silicalite-1. *J. Catal.* **157**(2), 482–500 (1995).
75. Efimov, A. M., Pogareva, V. G. & Shashkin, A. V. Water-related bands in the IR absorption spectra of silicate glasses. *J. Non-Cryst. Solids* **332**(1–3), 93–114 (2003).
76. Efimov, A. M. & Pogareva, V. G. IR absorption spectra of vitreous silica and silicate glasses: The nature of bands in the 1300 to 5000 cm—1 region. *Chem. Geol.* **229**(1–3), 198–217 (2006).
77. Asemani, M. & Rabbani, A. R. Detailed FTIR spectroscopy characterization of crude oil extracted asphaltenes: Curve resolve of overlapping bands. *J. Petrol. Sci. Eng.* **185**, 106618 (2020).
78. Ovchinnikov, O. V. et al. Manifestation of intermolecular interactions in FTIR spectra of methylene blue molecules. *Vib. Spectrosc.* **86**, 181–189 (2016).
79. Prasad, P. S. R. & Sarma, L. P. A near-infrared spectroscopic study of hydroxyl in natural chondrodite. *Am. Miner.* **89**(7), 1056–1060 (2004).
80. Zhang, Y. et al. Zeta potential: A surface electrical characteristic to probe the interaction of nanoparticles with normal and cancer human breast epithelial cells. *Biomed. Microdev.* **10**(2), 321–328 (2008).
81. Bhattacharjee, S. DLS and zeta potential—What they are and what they are not?. *J. Control. Release* **235**, 337–351 (2016).
82. Moslemizadeh, A., Shadizadeh, S. R. & Moomenie, M. Experimental investigation of the effect of henna extract on the swelling of sodium bentonite in aqueous solution. *Appl. Clay Sci.* **105–106**, 78–88 (2015).
83. Moslemizadeh, A. et al. Assessment of swelling inhibitive effect of CTAB adsorption on montmorillonite in aqueous phase. *Appl. Clay Sci.* **127–128**, 111–122 (2016).

Acknowledgements

The authors extend their appreciation to the Deanship of Research and Graduate Studies at King Khalid University for funding this work through Large Research Project under grant number RGP2/215/46.

Author contributions
All authors contributed equally to this research paper.

Declarations

Competing interests
The authors declare no competing interests.

Additional information
Correspondence and requests for materials should be addressed to Y.L. or S.S.

Reprints and permissions information is available at www.nature.com/reprints.

Publisher's note Springer Nature remains neutral with regard to jurisdictional claims in published maps and institutional affiliations.